Mast cell toll-like receptor 2 signaling is crucial for effective killing of *Francisella tularensis*[1]

Annette R. Rodriguez[*,†], **Jieh-Juen Yu**[*], **M. N. Guentzel**[*], **Christopher S. Navara**[*], **Karl E. Klose**[*], **Thomas G. Forsthuber**[*], **James P. Chambers**[*], **Michael T. Berton**[+], and **Bernard P Arulanandam**[*]

[*]University of Texas at San Antonio, South Texas Center for Emerging Infectious Diseases and Center of Excellence in Infection Genomics; San Antonio, Texas, 78249; USA

[†]St. Jude Children's Research Hospital, Department of Immunology; Memphis, TN, 38105; USA

[+]University of Texas Health Science Center at San Antonio, Department of Immunology and Microbiology; San Antonio, Texas, 78229; USA

Abstract

Toll-like receptor (TLR) signaling is critical for early host defense against pathogens, but the contribution of mast cell TLR-mediated mechanisms and subsequent effector functions during pulmonary infection is largely unknown. We have previously demonstrated that mast cells, through the production of IL-4, effectively control *Francisella tularensis* replication. In this study, the highly human virulent strain of *F. tularensis* SCHU S4 and the Live Vaccine Strain (LVS) were utilized to investigate the contribution of mast cell-TLR regulation of *Francisella*. Mast cells required TLR2 for effective bacterial killing, regulation of the hydrolytic enzyme cathepsin L, and for coordination and trafficking of MHCII and lysosomal associated membrane protein 2 (LAMP2). Infected TLR2$^{-/-}$ mast cells, in contrast to WT and TLR4$^{-/-}$, lacked detectable IL-4 and displayed increased cell death with a 2–3 log increase of *F. tularensis* replication, but could be rescued with recombinant IL-4 treatment. Importantly, MHCII and LAMP2 localization with labeled *F. tularensis* in the lungs was greater in WT than in TLR2$^{-/-}$ mice. These results provide evidence for the important effector contribution of mast cells and TLR2-mediated signaling on early innate processes in the lung following pulmonary *F. tularensis* infection and provide additional insight into possible mechanisms by which intracellular pathogens modulate respiratory immune defenses.

INTRODUCTION

Mast cells act as sentinels that sense bacterial products via host surface pattern recognition receptors such as toll-like receptor (TLR)2 and TLR4 (1, 2). While mast cell cytokine production following TLR recognition has been well documented (3–7), much is still unknown about mast cell TLR signaling and function during bacterial infection. In dendritic cells, TLR signaling triggers bacterial phagocytosis and promotes phagosome maturation, which entails nascent phagosome fusion with endosomes and phagolysosomal formation (8). Phagocytosis, phagosome maturation (9), and phagosome movement along microtubules to

[2]Corresponding Author: Bernard P. Arulanandam, South Texas Center for Emerging Infectious Disease and Center for Excellence in Infection Genomics, University of Texas at San Antonio, One UTSA Circle, San Antonio, TX 78249 phone 210.458.5492 fax 210.458.5523 bernard.arulanandam@utsa.edu.

perinuclear regions requires optimal pH regulation (10, 11). Although the maturation process has been studied in dendritic cells (8, 12, 13), the contribution of TLR function in mast cell phagocytosis is yet to be elucidated.

Phagosome maturation in myeloid lineage cells is marked by protein accumulation including CD63 (14), LAMP1/2 (15) and Rab7 (16, 17). Additional proteins in this process include the V-type ATPase, the major histocompatibility complex II (MHCII), and lysosomal hydrolases. To this end, lysosomal hydrolases are comprised of several cathepsins such as serine, aspartate and cysteine proteases (18–20). Among the cathepsins, cathepsin L is critical for cellular homeostasis, autophagy, apoptosis, and antigen processing and presentation (21, 22). Importantly, this protease also has been implicated in various diseases including diabetes (23), cancer (24), and lung inflammation (25) and, therefore, must be expediently regulated to maintain homeostasis.

Under ideal conditions, phagosome-lysosome fusion leads to a decrease in pH and protease activation which culminates in killing of pathogens within the phagolysosome. However, a number of pathogens have developed evasion mechanisms by modifying the phagosome or maturation events. For example, *Mycobacterium* spp. blocks the Rab5 positive stage (26), *Leishmania* spp. inhibits phagosome maturation (27), and *Coxiella burnetii* converts the phagosome into a hybrid autophagosome (28). *Francisella tularensis*, the causative agent of pneumonic tularemia, has been shown to escape the phagosome to evade lysosomal degradation and undergoes extensive replication within the macrophage cytosol (29).

Toll-like receptor 2 signaling and ensuing immune responses are important for the control of pulmonary *F. tularensis* (30). While TLR2 has been shown to be involved in recognition of *Francisella* lipoproteins (30–32), wild-type (WT), TLR2$^{-/-}$ and TLR4$^{-/-}$ macrophages have been shown to exhibit similar susceptibility to *F. tularensis* infection. We have recently shown that mast cells are essential for host survival during pulmonary *F. tularensis* challenge, and that mast cells co-cultured with macrophages promote killing of the organism via IL-4 secretion (33) and increased macrophage cellular ATP production with subsequent acidification (34).

Although cellular acidic conditions have been shown to control trafficking along microtubules (10, 35), and Yates and Russell (36) have shown that macrophage TLR2/4 signaling is not required for phagosome maturation, there is a paucity of information on mast cell TLR function and control of cellular trafficking and lysosomal function. Accordingly, using the highly human virulent strain of *F. tularensis* (SCHU S4) and *F. tularensis* Live Vaccine Strain (LVS), we investigated the contribution of mast cell TLR2/4 and IL-4 production to killing by mast cells. Our findings show that mast cell TLR2 is critical for optimal trafficking of cellular proteins and effective host responses during *Francisella* infection.

MATERIALS AND METHODS

Mice

Specific pathogen-free 4–8 week old mice were utilized for all procedures. C57BL/6 mice were purchased from the National Cancer Institute. TLR2$^{-/-}$ (37) and TLR4$^{-/-}$ (38) mice were provided by Dr. M. T. Berton. All experimental procedures and animal care were performed in accordance with the Institutional Animal Care and Use Committee (IACUC) guidelines.

Bacteria

Francisella tularensis LVS (obtained from Dr. R. Lyons at University of New Mexico), *F. tularensis* SCHU S4 (obtained from the Centers for Disease Control) and mCherry LVS KKF314) were grown in tryptic soy broth supplemented with L-cysteine (33). Experiments using SCHU S4 were conducted in a licensed ABSL-3 facility.

Generation of primary cells and *in vitro* infection

Mast cells were derived from mouse bone marrow and infected *in vitro* as described previously (33). Briefly, cells were counted, plated, and incubated for a 4 h rest period without cytokines prior to infection. Cells were then infected for 2 h, treated with gentamicin for 1 h, washed, incubated at 37 °C, and analyzed at various time-points. At 3, 12, or 24 h post-challenge with LVS (MOI 100) or *F. tularensis* SCHU S4 (MOI 100), bacteria were dilution plate counted using cellular lysates. In separate experiments, murine recombinant IL-4 (rIL-4, 5 or 25 ng/ml, eBioscience) was added to cell cultures 2 h prior to infection and rIL-4 was replaced after each wash step. Cells were used for determination of bacterial replication and protein expression.

In vivo challenge and flow cytometry

Six to eight week old C57/B6 and TLR2$^{-/-}$ mice were challenged i.n. with either 1 or 10 LD$_{50}$ of LVS or with PBS (mock challenge). At days 2 and 4 post-challenge, mice were euthanized. The lungs were perfused with 1X PBS and strained through a 70 μm cell strainer, or formalin was injected into the trachea and the lungs were fixed in neutral formalin overnight, dehydrated, and embedded in paraffin. Serial sections of 5 μm thickness were prepared. Tissue sections were permeabilized with 1X PermWash™ and blocked with BSA or rat serum. Tissues were stained for 45 min at room temperature with fluorochrome conjugated antibodies including anti-CD117, anti-LAMP2, anti-CD49b, anti-CD11c, or anti-F480 (BD Biosciences), and DAPI. Lung cells were washed with 2 % FBS in 1X PBS with 0.09 % sodium azide (PBS wash), then blocked with 10 % rat serum in 1X PBS at 4 °C for 30 minutes. Samples were washed and surfaced stained with appropriate fluorochrome conjugated antibody or isotype control, incubated at 4 °C for 30 min, and washed. Samples were then fixed in Cytofix/Cytoperm™ for 20 min, washed with PBS, and treated with 1X PermWash™ for 10 min, and the wash was removed. Cells were then stained with fluorochrome conjugated antibody or isotype control diluted in 100 μL 1X PermWash™ and added to appropriate samples. Samples were then incubated for 60 min with intermittent agitation, washed in 1X PermWash™, and resuspended in 2 % (w/v) paraformaldehyde for flow cytometer (FACSCalibur, BD Biosciences) analysis. Analyses were performed using CellQuest Pro software (BD Biosciences). Lung tissues also were examined using a 510 Meta (Zeiss) confocal microscope and data analyzed using Imaris software (Bitplane Inc.).

For *in vitro* analysis of mast cells and co-cultures, cells were collected at 15, 30, and 60 min, 3, 12, or 24 h and washed with PBS. Samples were subsequently blocked with anti-mouse CD16/CD32 (BD Biosciences), or with 10 % rat serum at 4 °C, followed by addition of fluorescent conjugated antibodies for surface and/or intracellular staining as noted above. Fluorescent antibodies included FcRI (phycoerythrin, PE), c-Kit fluorescein isothiocyanate (FITC) (Clone 2B8, eBioscience), CD11b (FITC or APC, allophycocyanin), CD206 (Clone MR5D3, BioLegend), or isotype controls (IgG1 PE, IgG2aκ FITC, IgG2aκ APC, IgG2aκ Alexa 488). For indirect staining of cathepsin L, secondary antibody with fluorochrome conjugated Alexa488 or Texas Red was used. Gating for analyses included side scatter versus c-Kit for primary mast cells, or CD11b for macrophages. Analysis of data was performed using CellQuest Pro software (BD Biosciences).

Microscopy

Lucifer yellow labeled bacteria were used for *in vitro* infection as described above; however, mast cells were cultured in polystyrene tubes or with 10 % RPMI containing 0.1 % gelatin (stabilization for tracking) in a 35 mm Ibidi μdish (Munich, Germany) for live imaging. For analysis of acidification (39), a specific acidification probe (LysoTracker Red DND-99, Invitrogen, Eugene, OR) was added to cultures and incubated for 30 min at 37 °C prior to infection. Lucifer yellow labeled LVS was added and cells were collected and stained at designated intervals as previously described for surface staining, followed by fixing, permeabilization and intracellular staining for 2 h at RT. A CytoPro was used at 800 rpm for 4 min to collect the cells on Poly-L-Lysine coated slides. Permount was added to the slides, coverslips were placed, and slides dried overnight at RT in the dark. Samples were examined using a confocal microscope (Zeiss 510 Meta, Carl Zeiss Microimaging Inc., Thornwood, NY), and analyzed with Imaris software (Bitplane Inc., St. Paul MN). For live cell imaging of WT and TLR2$^{-/-}$ mast cells, the Personal Deltavision fluorescent deconvolution microscope was used with either a 60 or 100X high numerical aperture objective. During acquisition of images, cells were maintained at 37 °C with 5 % CO_2 with acquisition of images at 60 sec intervals.

Confocal microscopy was employed for lung tissue analysis using a Zeiss LSM 510 confocal microscope. Lasers and settings for detection of fluorophores included: 405 for detection of DAPI BP 420–480), 488 for detection of Alexa 488 (NFT 490 and BP 505–530), 594 for detection of mCherry (NFT 545 and BP 560–615), and 633 for detection of APC (NFT 545 and LP 650).

Statistics

Data were analyzed by Student's t-test using the statistical software program SigmaStat Chicago, IL). A *P* value of 0.05 or less was considered statistically significant. Results are representative of at least two independent experiments.

RESULTS

Wild-type and TLR4$^{-/-}$ mast cells effectively control *Francisella* replication, while TLR2$^{-/-}$ mast cells are permissive to *Francisella* replication

Toll-like receptor 2 deficient (TLR2$^{-/-}$) mice have been shown to exhibit higher mortality than wild-type mice following *F. tularensis* pulmonary challenge (30, 32). Given that WT, TLR2$^{-/-}$ and TLR4$^{-/-}$ macrophages exhibit similar susceptibility to *Francisella*, and that we have previously shown that mast cells are important for bacterial control and survival during pulmonary *F. tularensis* infection (33), we compared replication in WT and TLR deficient mast cells during *Francisella* infection. Bacterial replication was examined at 3 and 24 h in WT mast cells infected with LVS and the highly human virulent type A strain, SCHU S4, and compared to infected TLR2$^{-/-}$ and TLR4$^{-/-}$ mast cells. These analyses revealed that while bacterial replication of both LVS and SCHU S4 was restricted in WT and TLR4$^{-/-}$ mast cells, TLR2$^{-/-}$ mast cells exhibited significantly (P<0.002) increased (2–3 log) replication compared to WT mast cells at 24 h (Fig. 1). Macrophages were used for comparison, and as previously observed (33, 34), LVS and SCHU S4 replicated robustly within primary WT macrophages. These results suggest that TLR2 recognition of bacteria and/or TLR2 signaling is critical for the control of *F. tularensis* replication within mast cells.

TLR2$^{-/-}$ mast cells lack detectable IL-4 production and exhibit reduced cathepsin L activation immediately following infection

Given that we have previously demonstrated that IL-4 is critical for mast cell inhibition of *F. tularensis* replication (33), and that TNF-α has been suggested to be an important innate

immune component in host defense (40, 41), supernatants collected from WT, TLR2$^{-/-}$ and TLR4$^{-/-}$ mast cells during mock or LVS infection were analyzed for IL-4 and TNF-α production. Both IL-4 and TNF-α were produced by LVS infected WT and TLR4$^{-/-}$ mast cells; whereas, TLR2$^{-/-}$ mast cells lacked detectable IL-4 production, but produced similar levels of TNF-α to WT mast cells (Fig. 2A). LVS-infected TLR4$^{-/-}$ mast cells exhibited marked reduction of TNF-α production compared with WT and TLR2$^{-/-}$ mast cells (Fig. 2A). Given that LVS or SCHU S4 infected TLR2$^{-/-}$ mast cells exhibited marked susceptibility to the organisms, but impaired IL-4 production in contrast to WT or TLR4$^{-/-}$ mast cells, additional studies were focused on the contribution of TLR2.

Since IL-4 treatment increases phagosome acidification during *Francisella* infection (34), and the hydrolytic protein cathepsin L has been shown to be enhanced by IL-4 (42), we subsequently analyzed the expression of cathepsin L by flow cytometry. These analyses revealed reduced active cathepsin L expression in TLR2$^{-/-}$ LVS-infected mast cells (55.0 %, representative histogram shown) at early time points (30 min shown; filled lines) compared to WT (Fig. 2B; 86.0 %, representative histogram shown). However, by one hour post LVS challenge (hatched lines), cathepsin L decreased in WT (Fig. 2 B; 12.5 %, representative histogram shown), and increased in TLR2$^{-/-}$ mast cells (95 %, representative histogram shown). Together, these results suggest that TLR2 recognition of *Francisella* and downstream signaling are important for IL-4 production and subsequent regulation of cathepsin L synthesis in mast cells.

TLR2$^{-/-}$ mast cells express altered LAMP and MHCII trafficking and acidification during *F. tularensis* infection

Since IL-4 has been shown to upregulate MHCII expression and acidification in macrophages (34, 43), and given that accumulation of the lysosomal associated membrane protein (LAMP2) is important during phagosome maturation and ensuing phagosome-lysosome fusion (21, 44), MHCII and LAMP2 were examined in Lucifer yellow labeled LVS infected WT, TLR2$^{-/-}$ and TLR4$^{-/-}$ mast cells. Flow cytometry analysis of MHCII surface expression during early (30 min) LVS infection revealed that WT mast cells express reduced MHCII surface proteins (22 %) compared to TLR2$^{-/-}$ mast cells, which expressed almost twice (41 %) the level and were comparable to TLR4$^{-/-}$ mast cells (37 %) [Fig. 3A]. We then utilized confocal microscopy to examine the relationship between MHCII and colocalization with labeled LVS. Interestingly, confocal microscopy analysis revealed that while TLR2$^{-/-}$ mast cells showed high levels of MHCII expression at the cell surface, intracellular MHCII expression was markedly reduced and greater numbers of LVS were present in the TLR2$^{-/-}$ mast cells, in contrast to WT mast cells which showed high levels of intracellular MHCII along with reduced Lucifer labeled bacteria (Fig. 3B). For further examination, we utilized 3-D confocal microscopy analysis at a higher magnification (1000X), and visualized notable aggregation of MHCII molecules with LAMP2 positive proteins in WT mast cells early (30 min) during LVS infection, in contrast to TLR2$^{-/-}$ mast cells with dispersed MHCII and LAMP2 positive proteins throughout the cells (Fig. 4A). However, by 3 h LAMP2 and MHCII trafficking to the cell surface increased, along with decreased c-Kit positive fluorescent proteins in TLR2$^{-/-}$ mast cells, when compared to WT mast cells (Fig. 4B). Moreover, increased levels of Lucifer yellow labeled bacteria in TLR2$^{-/-}$ mast cells also were noted compared to WT mast cells (Fig. 4B) which was in agreement with bacterial plate counts (Fig. 4C). Since TLR2$^{-/-}$ mast cells exhibited increased LVS replication and reduced colocalization with MHCII and acidification marker, we analyzed cell death by examining active caspase-3 induction as well as the effect of rIL-4 on these processes. Importantly, LVS and SCHU S4 infected TLR2$^{-/-}$ mast cells exhibited a significant increase in active caspase-3 expression when compared to similarly infected WT or TLR4$^{-/-}$ mast cells (Fig. 4C, only SCHU S4 shown), while addition of rIL-4 to the

TLR2$^{-/-}$ mast cells reduced active caspase-3 induction and conferred control of SCHU S4 bacterial replication similar to WT mast cells. These results suggest that mast cell TLR2 recognition of *F. tularensis* and consequential downstream signaling promote phagosome maturation, trafficking of LAMP2 and MHCII molecules, and killing of *Francisella*, which is likely related to IL-4 signaling. Addition of rIL-4 rescued SCHU S4-infected TLR2$^{-/-}$ mast cells from apoptosis and promoted effective killing of the organism.

The infiltration and localization of mast cells with mCherry labeled LVS following pulmonary infection

Given the striking *in vitro* differences between WT and TLR2 deficient mast cells during *F. tularensis* infection, we analyzed the early cellular events as well as mast cell migration to the lungs following pulmonary challenge. C57BL/6 mice were challenged (10 LD$_{50}$) i.n. with mCherry labeled LVS and lungs were collected at days 2 and 4 post-challenge. At day 2 post challenge, minimal c-Kit positive cells were noted (data not shown); in agreement with our previous study (33). However, cellular infiltration to the lungs was evident by day 4 post challenge. Concurrently, analysis of lung tissue collected from LVS challenged WT mice revealed notable aggregated LAMP2 molecules that encompassed mCherry labeled LVS when compared to lung tissue from TLR2$^{-/-}$ challenged mice by day 4 (Fig. 5A). Moreover, the intensity of Lamp staining within these regions was greater in the WT compared to TLR2$^{-/-}$ lung sections (Fig. 5B).

Since subpopulations of dendritic cells and natural killer cells (NK cells) have been reported to express c-Kit, lung cells were analyzed for c-Kit expression in addition to CD49b (a pan-NK cell marker) and CD11c (dendritic cell marker; Fig. 6). Flow cytometry analyses of WT lung cells collected from mock and mCherry labeled LVS challenged mice revealed that cells expressing c-Kit during pulmonary *F. tularensis* challenge primarily consisted of mast cells and natural killer cells. At day 4 post-challenge, approximately 26 % of lung cells were c-Kit positive; 65 % of this c-Kit population also were FcεRI positive, indicative of mast cells, and 8.5 % were CD49b positive, indicative of cytotoxic NK cells (Fig. 6A–B). Importantly, lung cell analyses also indicated that c-Kit positive cells interact with *Francisella* during pulmonary infection (Fig. 6C); although, minimal mCherry cKit positive cells were noted (insert-higher magnification). Since wild-type mast cells are not permissive to *F. tularensis* replication, live cell imaging was used in order to further analyze the WT and TLR2$^{-/-}$ mast cell-*Francisella* interaction. Live cell imaging (Video 1, legend in Supplemental Data) demonstrated that WT mast cells were polarized, highly mobile, and efficient in killing of Lucifer-labeled LVS in contrast to TLR2$^{-/-}$ mast cells. Furthermore, live cell imaging of TLR2$^{-/-}$ mast cells (Video 2, legend in Supplemental Data) demonstrated that the cells efficiently engulf Lucifer yellow labeled LVS (green); however, bacteria did not localize within acidified regions (red), and instead persist (green) within the mast cells. Sequential images of WT mast cells (Supplemental Fig. S1A–D) show polarized acidification regions (white arrows) during phagocytosis of bacteria, in contrast to TLR2$^{-/-}$ mast cells with acidification regions around the mast cell periphery (white arrows, Supplemental Fig. S1E–H lower panel). Collectively, the live cell imaging of WT mast cell (Video 1), revealed rapid phagocytosis, acidification (red) and degradation of LVS (green) suggestive of a more efficient phagosome and phago-lysosomal maturation process. Importantly, these results are in agreement with bacterial plate count information showing that TLR2$^{-/-}$ mast cells efficiently engulf *Francisella*, but permit survival and growth of the organisms; whereas, WT mast cells demonstrate effective killing of the pathogen.

DISCUSSION

Mast cells provide a dynamic defense against mucosal pathogens. Control of certain bacterial pulmonary pathogens, including *F. tularensis* (30, 32, 45), *Mycobacterium*

tuberculosis (46) and *Pseudomonas aeruginosa* (47, 48), requires TLR2 receptor signaling. This study provides further mechanistic insight into mast cell bacterial recognition and control of infection.

Importantly, mast cell TLR2-mediated innate immune responses included optimal trafficking and early accumulation of LAMP2, MHCII, and cathepsin L which resulted in effective killing of *F. tularensis*. Toll-like receptor signaling and subsequent lysosomal function have been primarily characterized in dendritic cells (49). Trombetta and colleagues used LPS to demonstrate that mature dendritic cells accumulate vacuolar pumps resulting in enhanced acidified lysosomes and antigen proteolysis (Trombetta et al., 2003). These dendritic cells also were shown to accumulate MHCII molecules. Blander and Medzhitov later demonstrated that dendritic cell TLR4 recognition of LPS is critical for phagosome maturation and discrimination of self (apoptotic cells) and non-self for antigen presentation (50). In contrast, Yates and Russell have proposed that phagosome maturation occurs independently of TLR2 or TLR4 stimulation, using bone marrow derived macrophages stimulated with Pam3CysSerLys (synthetic lipoprotein) or LPS (36). Although there may be multiple differences in the *in vitro* systems noted above, IL-4 was a principle component required for mast cell activity in our study. We previously have demonstrated that bone marrow derived macrophages are highly permissive to *Francisella* infection; however, co-culture with mast cells or the addition of rIL-4 markedly reduced bacterial replication (33, 34). Importantly, it should be noted that bone marrow derived macrophages did not produce IL-4 during infection in contrast to bone marrow derived mast cells. We also have provided evidence that in mast cell-macrophage co-culture, the production of IL-4 by mast cells promotes macrophage ATP production and subsequent phagosome acidification (34). Therefore, the differences noted by Yates and Russell (36) may have been partially due to the lack of IL-4 production by macrophages.

Previous studies (51–53) have shown that interferon-γ and TNF-α are primary control mechanisms during *Francisella* infection. While addition of IFN-γ also improved killing of LVS in mast cells and increased IL-4 production (data not shown), TNF-α was not sufficient to induce *Francisella* killing in mast cells as demonstrated by TLR2$^{-/-}$ mast cells, which produced comparable levels to WT mast cells. Although, reactive oxygen species (ROS) induced by TNF-have been shown to promote signaling via the IL-4 receptor pathway, TNF-α is not required for initiation of IL-4 signaling (54). IL-4 enhances ATP production (55), cathepsin L activation (42), and phagosome acidification (34). Additionally, our findings suggest that TLR2 signaling was required for induction of mast cell IL-4 secretion, optimal cathepsin L activation, and phagosome maturation resulting in localization of LAMP2 and MHCII molecules with *F. tularensis*. It has previously been demonstrated that BMDMC from WT and TLR4$^{-/-}$ mice produced similar levels of both TNF-α and IL-4 when stimulated with peptidoglycan from *Staphylococcus aureus*, whereas similarly stimulated TLR2$^{-/-}$ mast cells produced neither cytokine (56). This is in agreement with our observation of the lack of IL-4 in *Francisella*-infected TLR2$^{-/-}$ mast cells. The observed TNF-α production within TLR2$^{-/-}$ mast cells may be attributed by the induction of other TLRs including TLR4. Importantly, TLR2 signaling has been reported to link phagocytosis to autophagy and requires acidification (57, 58). To this end, the seminal work of Heuser (35) demonstrated that cellular acidic and alkaline conditions influence lysosome trafficking along microtubules. Our findings suggest that cathepsin L activity, which targets multiple cellular proteins implicated in trafficking such as dynamin (59) and actin (60), must also be regulated in a manner for efficient movement and maturation of the phagosome-lysosome to ensure destruction of *Francisella*, as overexpression is associated with induction of apoptosis and tissue damage (24, 61). Furthermore, TLR2 signaling has been reported to be important for control of *M. tuberculosis* (46). Effective control of this pathogen also may be dependent on ensuing acidification required for TLR9 conformational changes and subsequent function

(62). Results from work reported here support a probable link for TLR2 signaling and ensuing acidification for TLR9 function.

Given that early TLR2 signaling and phagosome maturation were key to efficient mast cell bacterial killing, this study provides additional avenues to exploit in control of intracellular bacterial pathogens. TLR2 signaling and IL-4 production resulted in early enhanced levels of active cathepsin L, which is important for cleavage of the invariant chain (20, 63). Additionally, IL-4 is associated with the production of cathepsin B and S which may be involved in development of cancers (64), while extracellular cathepsin L has been implicated in apoptosis (61), tissue damage and tumorigenesis (24, 65). TLR2$^{-/-}$ mast cells demonstrated an excess of active cathepsin L compared to WT after 1 h of LVS infection as demonstrated by confocal microscopy and flow cytometry. Confocal microscopy analyses also showed disintegration of the mast cell plasma membrane and release of LVS. Intense LAMP2 and cathepsin L positive regions at the membrane of TLR2$^{-/-}$ mast cells, along with numerous Lucifer yellow labeled LVS and diminished or undetectable c-Kit proteins, suggest that lysosomes were localized at the plasma membrane contributing to the destruction of membrane integrity. To this end, it has previously been shown that lysosomes localize at the plasma membrane for repair processes following initial translocation of phosphatidyl serine to the outer surface of the membrane (66). This repair process requires an increase of calcium and actin polymerization, and bacteria may take advantage of the process (67, 68) for escape into the extracellular region, demonstrating the critical requirement for stringent mast cell TLR2 regulation. In summary, this study provides additional mechanistic insight into mast cell mediated innate immune mechanisms and the positive contribution of this cell type during pulmonary infection with Gram negative bacteria.

Supplementary Material

Refer to Web version on PubMed Central for supplementary material.

Acknowledgments

Abbreviations

LAMP2	Lysosomal associated membrane protein 2
LVS	Live Vaccine Strain

REFERENCES

1. McCurdy JD, Lin TJ, Marshall JS. Toll-like receptor 4-mediated activation of murine mast cells. J. Leukoc. Biol. 2001; 70:977–984. [PubMed: 11739561]

2. Supajatura V, Ushio H, Nakao A, Okumura K, Ra C, Ogawa H. Protective roles of mast cells against enterobacterial infection are mediated by Toll-like receptor 4. J. Immunol. 2001; 167:2250–2256. [PubMed: 11490012]

3. Gon Y, Nunomura S, Ra C. Common and distinct signalling cascades in the production of tumour necrosis factor-alpha and interleukin-13 induced by lipopolysaccharide in RBL-2H3 cells. Clin. Exp. Allergy. 2005; 35:635–642. [PubMed: 15898987]

4. Fehrenbach K, Port F, Grochowy G, Kalis C, Bessler W, Galanos C, Krystal G, Freudenberg M, Huber M. Stimulation of mast cells via FcvarepsilonR1 and TLR2: the type of ligand determines the outcome. Mol. Immunol. 2007; 44:2087–2094. [PubMed: 17095089]

5. Carlos D, Frantz FG, Souza-Junior DA, Jamur MC, Oliver C, Ramos SG, Quesniaux VF, Ryffel B, Silva CL, Bozza MT, Faccioli LH. TLR2-dependent mast cell activation contributes to the control of *Mycobacterium tuberculosis* infection. Microbes Infect. 2009; 11:770–778. [PubMed: 19442756]

6. McCurdy JD, Olynych TJ, Maher LH, Marshall JS. Cutting edge: distinct Toll-like receptor 2 activators selectively induce different classes of mediator production from human mast cells. J. Immunol. 2003; 170:1625–1629. [PubMed: 12574323]

7. Malaviya R, Ikeda T, Abraham SN. Contribution of mast cells to bacterial clearance and their proliferation during experimental cystitis induced by type 1 fimbriated *E. coli*. Immunol. Lett. 2004; 91:103–111. [PubMed: 15019277]

8. Blander JM, Medzhitov R. Regulation of phagosome maturation by signals from toll-like receptors. Science. 2004; 304:1014–1018. [PubMed: 15143282]

9. Vieira OV, Botelho RJ, Grinstein S. Phagosome maturation: aging gracefully. Biochem. J. 2002; 366:689–704. [PubMed: 12061891]

10. Blocker A, Griffiths G, Olivo JC, Hyman AA, Severin FF. A role for microtubule dynamics in phagosome movement. J. Cell Sci. 1998; 111(Pt 3):303–312. [PubMed: 9427679]

11. Moller W, Nemoto I, Matsuzaki T, Hofer T, Heyder J. Magnetic phagosome motion in J774A.1 macrophages: influence of cytoskeletal drugs. Biophys. J. 2000; 79:720–730. [PubMed: 10920006]

12. Sallusto F, Cella M, Danieli C, Lanzavecchia A. Dendritic cells use macropinocytosis and the mannose receptor to concentrate macromolecules in the major histocompatibility complex class II compartment: downregulation by cytokines and bacterial products. J. Exp. Med. 1995; 182:389–400. [PubMed: 7629501]

13. Trombetta ES, Ebersold M, Garrett W, Pypaert M, Mellman I. Activation of lysosomal function during dendritic cell maturation. Science. 2003; 299:1400–1403. [PubMed: 12610307]

14. Peters PJ, Borst J, Oorschot V, Fukuda M, Krahenbuhl O, Tschopp J, Slot JW, Geuze HJ. Cytotoxic T lymphocyte granules are secretory lysosomes, containing both perforin and granzymes. J. Exp. Med. 1991; 173:1099–1109. [PubMed: 2022921]

15. Cha Y, Holland SM, August JT. The cDNA sequence of mouse LAMP-2. Evidence for two classes of lysosomal membrane glycoproteins. J. Biol. Chem. 1990; 265:5008–5013. [PubMed: 2318880]

16. Chavrier P, Vingron M, Sander C, Simons K, Zerial M. Molecular cloning of YPT1/SEC4-related cDNAs from an epithelial cell line. Mol. Cell. Biol. 1990; 10:6578–6585. [PubMed: 2123294]

17. Chavrier P, Parton RG, Hauri HP, Simons K, Zerial M. Localization of low molecular weight GTP binding proteins to exocytic and endocytic compartments. Cell. 1990; 62:317–329. [PubMed: 2115402]

18. Kirschke H, Wood L, Roisen FJ, Bird JW. Activity of lysosomal cysteine proteinase during differentiation of rat skeletal muscle. Biochem. J. 1983; 214:871–877. [PubMed: 6354179]

19. Tulkens P, Trouet A, Van Hoof F. Immunological inhibition of lysosome function. Nature. 1970; 228:1282–1285. [PubMed: 4098956]

20. Bevec T, Stoka V, Pungercic G, Dolenc I, Turk V. Major histocompatibility complex class II-associated p41 invariant chain fragment is a strong inhibitor of lysosomal cathepsin L. J. Exp. Med. 1996; 183:1331–1338. [PubMed: 8666891]

21. Eskelinen EL, Illert AL, Tanaka Y, Schwarzmann G, Blanz J, Von Figura K, Saftig P. Role of LAMP-2 in lysosome biogenesis and autophagy. Mol. Biol. Cell. 2002; 13:3355–3368. [PubMed: 12221139]

22. Reinheckel T, Deussing J, Roth W, Peters C. Towards specific functions of lysosomal cysteine peptidases: phenotypes of mice deficient for cathepsin B or cathepsin L. Biol. Chem. 2001; 382:735–741. [PubMed: 11517926]

23. Maehr R, Mintern JD, Herman AE, Lennon-Dumenil AM, Mathis D, Benoist C, Ploegh HL. Cathepsin L is essential for onset of autoimmune diabetes in NOD mice. J. Clin. Invest. 2005; 115:2934–2943. [PubMed: 16184198]

24. Gocheva V, Zeng W, Ke D, Klimstra D, Reinheckel T, Peters C, Hanahan D, Joyce JA. Distinct roles for cysteine cathepsin genes in multistage tumorigenesis. Genes Dev. 2006; 20:543–556. [PubMed: 16481467]

25. Gerber A, Welte T, Ansorge S, Buhling F. Expression of cathepsins B and L in human lung epithelial cells is regulated by cytokines. Adv. Exp. Med. Biol. 2000; 477:287–292. [PubMed: 10849756]

26. Vergne I, Chua J, Singh SB, Deretic V. Cell biology of *Mycobacterium tuberculosis* phagosome. Annu. Rev. Cell Dev. Biol. 2004; 20:367–394. [PubMed: 15473845]

27. Scianimanico S, Desrosiers M, Dermine JF, Meresse S, Descoteaux A, Desjardins M. Impaired recruitment of the small GTPase rab7 correlates with the inhibition of phagosome maturation by *Leishmania donovani* promastigotes. Cell Microbiol. 1999; 1:19–32. [PubMed: 11207538]

28. Romano PS, Gutierrez MG, Beron W, Rabinovitch M, Colombo MI. The autophagic pathway is actively modulated by phase II *Coxiella burnetii* to efficiently replicate in the host cell. Cell Microbiol. 2007; 9:891–909. [PubMed: 17087732]

29. Lai XH, Sjostedt A. Delineation of the molecular mechanisms of *Francisella tularensis*-induced apoptosis in murine macrophages. Infect. Immun. 2003; 71:4642–4646. [PubMed: 12874344]

30. Abplanalp AL, Morris IR, Parida BK, Teale JM, Berton MT. TLR-dependent control of *Francisella tularensis* infection and host inflammatory responses. PLoS One. 2009; 4:e7920. [PubMed: 19936231]

31. Thakran S, Li H, Lavine CL, Miller MA, Bina JE, Bina XR, Re F. Identification of *Francisella tularensis* lipoproteins that stimulate the toll-like receptor (TLR) 2/TLR1 heterodimer. J. Biol. Chem. 2008; 283:3751–3760. [PubMed: 18079113]

32. Malik M, Bakshi CS, Sahay B, Shah A, Lotz SA, Sellati TJ. Toll-like receptor 2 is required for control of pulmonary infection with *Francisella tularensis*. Infect. Immun. 2006; 74:3657–3662. [PubMed: 16714598]

33. Ketavarapu JM, Rodriguez AR, Yu JJ, Cong Y, Murthy AK, Forsthuber TG, Guentzel MN, Klose KE, Berton MT, Arulanandam BP. Mast cells inhibit intramacrophage *Francisella tularensis* replication via contact and secreted products including IL-4. Proc. Natl. Acad. Sci. U. S. A. 2008; 105:9313–9318. [PubMed: 18591675]

34. Rodriguez AR, Yu JJ, Murthy AK, Guentzel MN, Klose KE, Forsthuber TG, Chambers JP, Berton MT, Arulanandam BP. Mast cell/IL-4 control of *Francisella tularensis* replication and host cell death is associated with increased ATP production and phagosomal acidification. Mucosal Immunol. 2010; 4:217–226. [PubMed: 20861832]

35. Heuser J. Changes in lysosome shape and distribution correlated with changes in cytoplasmic pH. J. Cell. Biol. 1989; 108:855–864. [PubMed: 2921284]

36. Yates RM, Russell DG. Phagosome maturation proceeds independently of stimulation of toll-like receptors 2 and 4. Immunity. 2005; 23:409–417. [PubMed: 16226506]

37. Takeuchi O, Hoshino K, Kawai T, Sanjo H, Takada H, Ogawa T, Takeda K, Akira S. Differential roles of TLR2 and TLR4 in recognition of gram-negative and gram-positive bacterial cell wall components. Immunity. 1999; 11:443–451. [PubMed: 10549626]

38. Hoshino K, Takeuchi O, Kawai T, Sanjo H, Ogawa T, Takeda Y, Takeda K, Akira S. Cutting edge: Toll-like receptor 4 (TLR4)-deficient mice are hyporesponsive to lipopolysaccharide: evidence for TLR4 as the Lps gene product. J. Immunol. 1999; 162:3749–3752. [PubMed: 10201887]

39. Griffiths G, Hoflack B, Simons K, Mellman I, Kornfeld S. The mannose 6-phosphate receptor and the biogenesis of lysosomes. Cell. 1988; 52:329–341. [PubMed: 2964276]

40. Cowley SC, Goldberg MF, Ho JA, Elkins KL. The membrane form of tumor necrosis factor is sufficient to mediate partial innate immunity to *Francisella tularensis* live vaccine strain. J. Infect. Dis. 2008; 198:284–292. [PubMed: 18593295]

41. Elkins KL, Cowley SC, Bosio CM. Innate and adaptive immunity to *Francisella*. Ann. N. Y. Acad. Sci. 2007; 1105:284–324. [PubMed: 17468235]

42. Van Den Berg JG, Aten J, Annink C, Ravesloot JH, Weber E, Weening JJ. Interleukin-4 and -13 promote basolateral secretion of H(+) and cathepsin L by glomerular epithelial cells. Am. J. Physiol. Renal Physiol. 2002; 282:F26–F33. [PubMed: 11739109]

43. Stein M, Keshav S, Harris N, Gordon S. Interleukin 4 potently enhances murine macrophage mannose receptor activity: a marker of alternative immunologic macrophage activation. J. Exp. Med. 1992; 176:287–292. [PubMed: 1613462]

44. Yates RM, Hermetter A, Russell DG. The kinetics of phagosome maturation as a function of phagosome/lysosome fusion and acquisition of hydrolytic activity. Traffic. 2005; 6:413–420. [PubMed: 15813751]

45. Cole LE, Santiago A, Barry E, Kang TJ, Shirey KA, Roberts ZJ, Elkins KL, Cross AS, Vogel SN. Macrophage proinflammatory response to *Francisella tularensis* live vaccine strain requires coordination of multiple signaling pathways. J. Immunol. 2008; 180:6885–6891. [PubMed: 18453609]

46. Underhill DM, Ozinsky A, Smith KD, Aderem A. Toll-like receptor-2 mediates mycobacteria-induced proinflammatory signaling in macrophages. Proc. Natl. Acad. Sci. U. S. A. 1999; 96:14459–14463. [PubMed: 10588727]

47. Soong G, Reddy B, Sokol S, Adamo R, Prince A. TLR2 is mobilized into an apical lipid raft receptor complex to signal infection in airway epithelial cells. J. Clin. Invest. 2004; 113:1482–1489. [PubMed: 15146246]

48. Raoust E, Balloy V, Garcia-Verdugo I, Touqui L, Ramphal R, Chignard M. *Pseudomonas aeruginosa* LPS or flagellin are sufficient to activate TLR-dependent signaling in murine alveolar macrophages and airway epithelial cells. PLoS One. 2009; 4:e7259. [PubMed: 19806220]

49. Blander JM, Medzhitov R. Toll-dependent selection of microbial antigens for presentation by dendritic cells. Nature. 2006; 440:808–812. [PubMed: 16489357]

50. Blander JM, Medzhitov R. On regulation of phagosome maturation and antigen presentation. Nat. Immunol. 2006; 7:1029–1035. [PubMed: 16985500]

51. Elkins KL, Cowley SC, Bosio CM. Innate and adaptive immune responses to an intracellular bacterium, *Francisella tularensis* live vaccine strain. Microbes Infect. 2003; 5:135–142. [PubMed: 12650771]

52. Collazo CM, Sher A, Meierovics AI, Elkins KL. Myeloid differentiation factor-88 (MyD88) is essential for control of primary in vivo *Francisella tularensis* LVS infection, but not for control of intra-macrophage bacterial replication. Microbes Infect. 2006; 8:779–790. [PubMed: 16513388]

53. Ray HJ, Cong Y, Murthy AK, Selby DM, Klose KE, Barker JR, Guentzel MN, Arulanandam BP. Oral live vaccine strain-induced protective immunity against pulmonary *Francisella tularensis* challenge is mediated by CD4+ T cells and antibodies, including immunoglobulin A. Clin. Vaccine Immunol. 2009; 16:444–452. [PubMed: 19211773]

54. Sharma P, Chakraborty R, Wang L, Min B, Tremblay ML, Kawahara T, Lambeth JD, Haque SJ. Redox regulation of interleukin-4 signaling. Immunity. 2008; 29:551–564. [PubMed: 18957266]

55. Dufort FJ, Bleiman BF, Gumina MR, Blair D, Wagner DJ, Roberts MF, Abu-Amer Y, Chiles TC. Cutting edge: IL-4-mediated protection of primary B lymphocytes from apoptosis via Stat6-dependent regulation of glycolytic metabolism. J. Immunol. 2007; 179:4953–4957. [PubMed: 17911579]

56. Supajatura V, Ushio H, Nakao A, Akira S, Okumura K, Ra C, Ogawa H. Differential responses of mast cell Toll-like receptors 2 and 4 in allergy and innate immunity. J. Clin. Invest. 2002; 109:1351–1359. [PubMed: 12021251]

57. Sanjuan MA, Dillon CP, Tait SW, Moshiach S, Dorsey F, Connell S, Komatsu M, Tanaka K, Cleveland JL, Withoff S, Green DR. Toll-like receptor signalling in macrophages links the autophagy pathway to phagocytosis. Nature. 2007; 450:1253–1257. [PubMed: 18097414]

58. Anand PK, Tait SW, Lamkanfi M, Amer AO, Nunez G, Pages G, Pouyssegur J, McGargill MA, Green DR, Kanneganti TD. TLR2 and RIP2 pathways mediate autophagy of *Listeria monocytogenes* via extracellular signal-regulated kinase (ERK) activation. J. Biol. Chem. 2011; 286:42981–42991. [PubMed: 22033934]

59. Touret N, Furuya W, Forbes J, Gros P, Grinstein S. Dynamic traffic through the recycling compartment couples the metal transporter Nramp2 (DMT1) with the transferrin receptor. J. Biol. Chem. 2003; 278:25548–25557. [PubMed: 12724326]

60. Gopaldass N, Patel D, Kratzke R, Dieckmann R, Hausherr S, Hagedorn M, Monroy R, Kruger J, Neuhaus EM, Hoffmann E, Hille K, Kuznetsov SA, Soldati T. Dynamin A, Myosin IB and Abp1 couple phagosome maturation to F-actin binding. Traffic. 2012; 13:120–130. [PubMed: 22008230]

61. Kidd VJ, Lahti JM, Teitz T. Proteolytic regulation of apoptosis. Semin. Cell Dev. Biol. 2000; 11:191–201. [PubMed: 10906276]

62. Rutz M, Metzger J, Gellert T, Luppa P, Lipford GB, Wagner H, Bauer S. Toll-like receptor 9 binds single-stranded CpG-DNA in a sequence- and pH-dependent manner. Eur. J. Immunol. 2004; 34:2541–2550. [PubMed: 15307186]

63. VanBuskirk AM, DeNagel DC, Guagliardi LE, Brodsky FM, Pierce SK. Cellular and subcellular distribution of PBP72/74, a peptide-binding protein that plays a role in antigen processing. J. Immunol. 1991; 146:500–506. [PubMed: 1987275]

64. Gocheva V, Wang HW, Gadea BB, Shree T, Hunter KE, Garfall AL, Berman T, Joyce JA. IL-4 induces cathepsin protease activity in tumor-associated macrophages to promote cancer growth and invasion. Genes Dev. 2010; 24:241–255. [PubMed: 20080943]

65. Amuthan G, Biswas G, Zhang SY, Klein-Szanto A, Vijayasarathy C, Avadhani NG. Mitochondria-to-nucleus stress signaling induces phenotypic changes, tumor progression and cell invasion. EMBO. J. 2001; 20:1910–1920. [PubMed: 11296224]

66. Stockinger W, Zhang SC, Trivedi V, Jarzylo LA, Shieh EC, Lane WS, Castoreno AB, Nohturfft A. Differential requirements for actin polymerization, calmodulin, and Ca2+ define distinct stages of lysosome/phagosome targeting. Mol. Biol. Cell. 2006; 17:1697–1710. [PubMed: 16452628]

67. Beatty WL. Lysosome repair enables host cell survival and bacterial persistence following *Chlamydia trachomatis* infection. Cell. Microbiol. 2007; 9:2141–2152. [PubMed: 17451410]

68. Roy D, Liston DR, Idone VJ, Di A, Nelson DJ, Pujol C, Bliska JB, Chakrabarti S, Andrews NW. A process for controlling intracellular bacterial infections induced by membrane injury. Science. 2004; 304:1515–1518. [PubMed: 15178804]
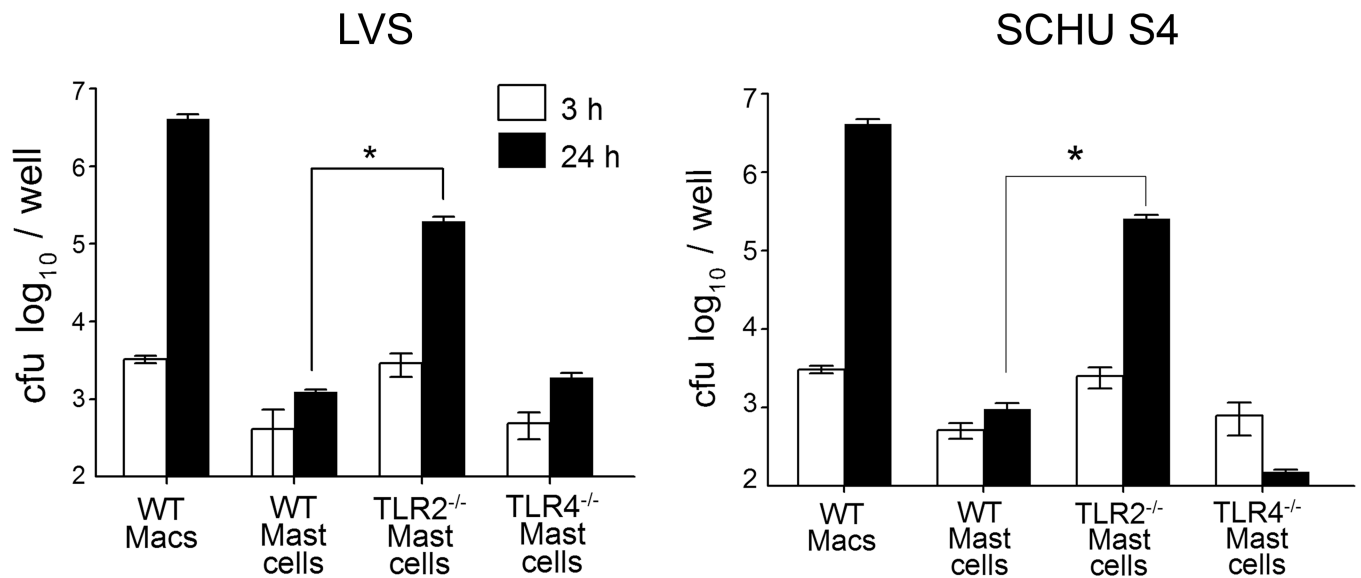
LVS   SCHU S4

Figure 1. TLR2$^{-/-}$ Mast cells are highly susceptible to *F. tularensis* infection
WT bone marrow derived mast cells (BMDMCs) were infected (100 MOI) with *F. tularensis*
LVS or SCHU S4 and compared to infected (100 MOI) TLR4$^{-/-}$ and TLR2$^{-/-}$ mast cells.
WT macrophages served as positive controls. Mast cell cultures were lysed at 3 (white) or
24 h (solid bar) with deoxycholate and lysates analyzed for bacterial replication. Unpaired t
test *P<0.002. Error bars represent the mean ±SD.
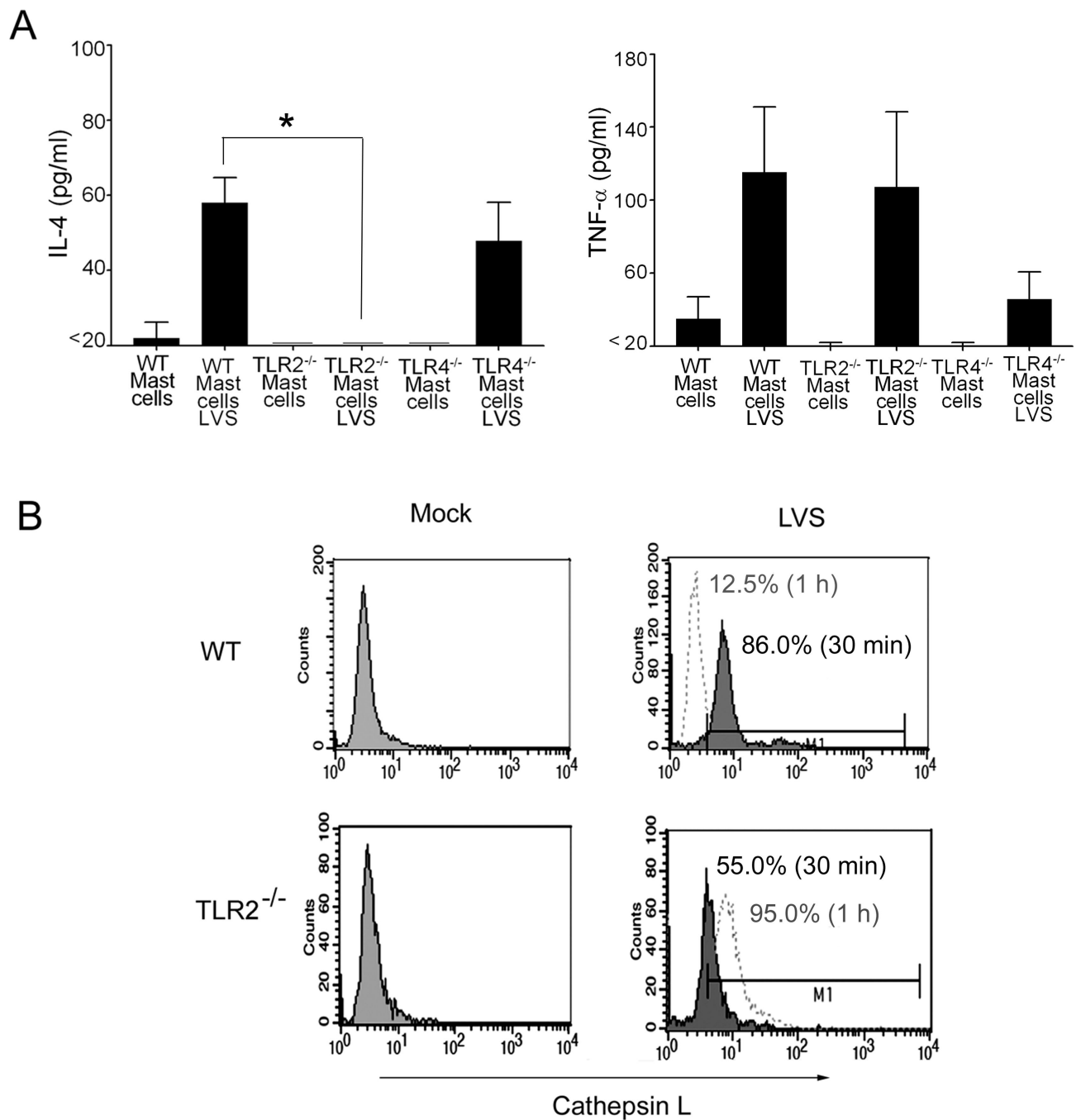
Figure 2. TLR2$^{-/-}$ mast cells lack detectable IL-4 production and exhibit reduced cathepsin expression immediately following *F. tularensis* infection
(A) Analysis of uninfected or LVS infected mast cells (WT, TLR2$^{-/-}$ and TLR4$^{-/-}$) for IL-4 and TNF-α production by ELISA. Unpaired t test *p<0.05. Error bars represent the mean ±SD. (B) Cathepsin L flow cytometric analysis at 30 min (filled line) and 1 hr (hatched line). Representative histograms are shown with isotype controls (left).
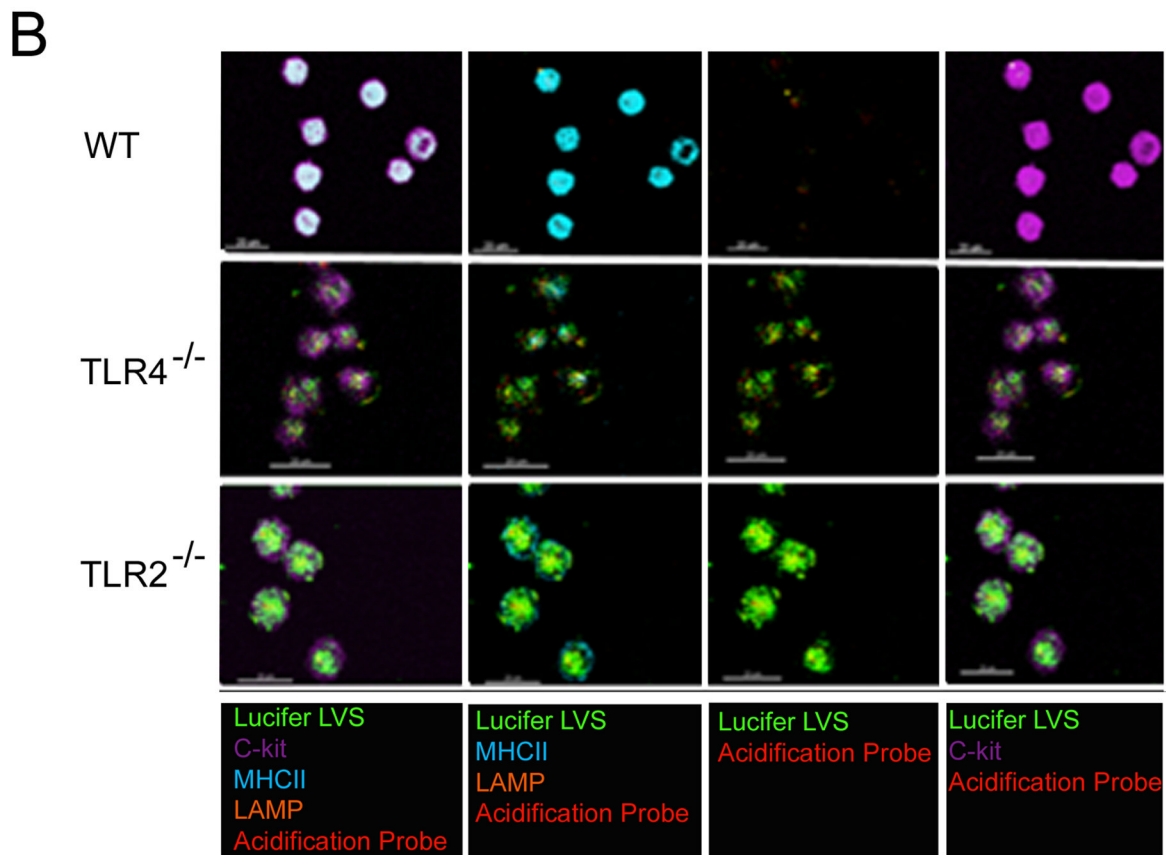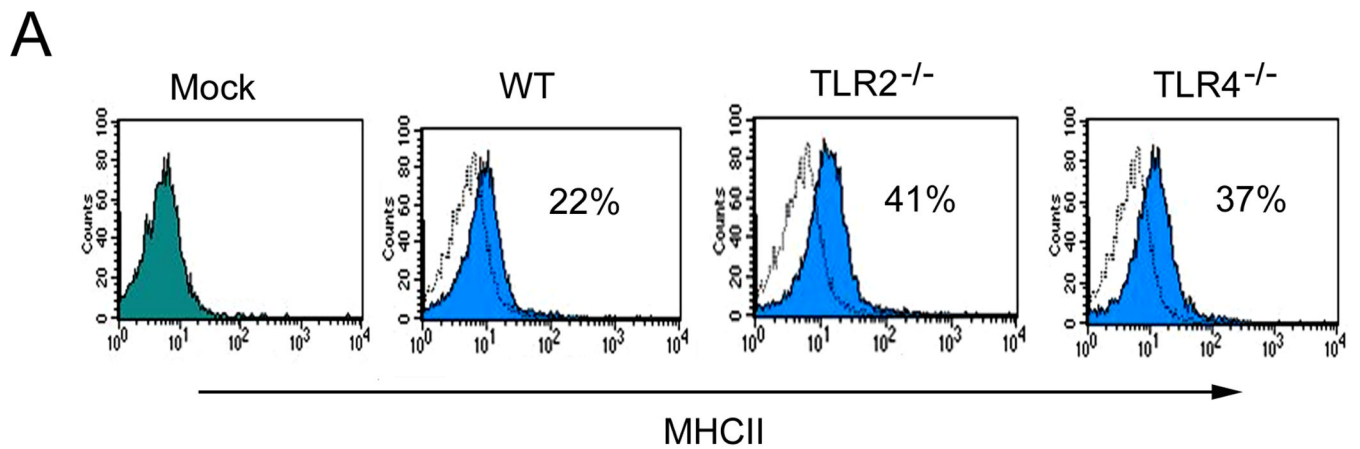
Figure 3. MHCII and LAMP2 expression are altered in TLR2$^{-/-}$ deficient mast cells
(A) WT, TLR2$^{-/-}$ and TLR4$^{-/-}$ mast cell MHCII surface analysis by flow cytometry. Representative histograms shown. (B) WT, TLR2$^{-/-}$ and TLR4$^{-/-}$ mast cells infected with Lucifer yellow labeled LVS (green) and labeled with c-Kit (purple) surface fluorescent conjugated antibody with intracellular MHCII (light blue), LAMP2 (orange), and acidification probe (red). Representative images shown at 30 min; 400X magnification.
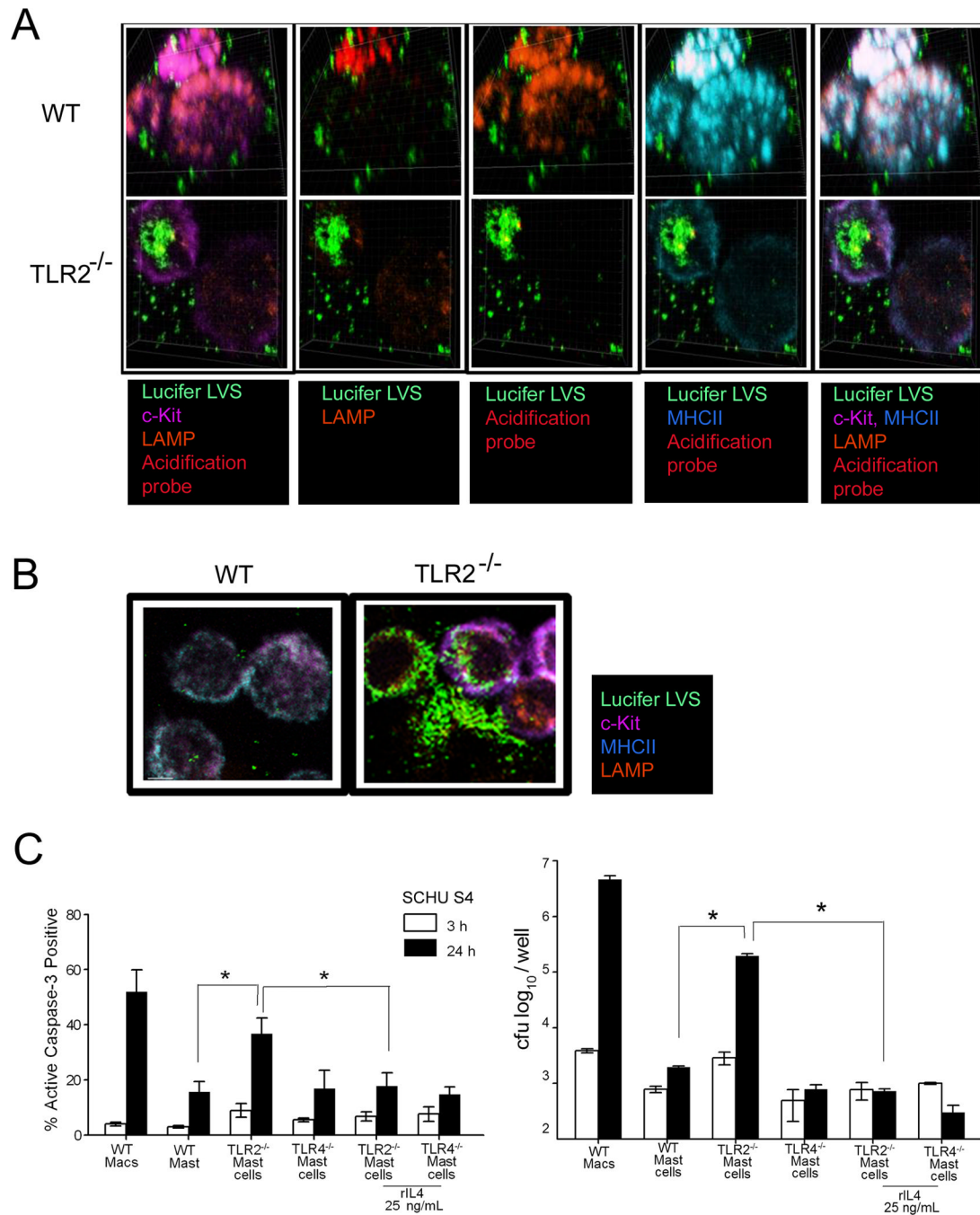
Figure 4. TLR2$^{-/-}$ deficient mast cells exhibit increased *F. tularensis* replication and cellular destruction
(A) WT and TLR2$^{-/-}$ mast cell analysis by confocal microscopy. Lucifer yellow labeled LVS (green); c-Kit (purple) surfaced labeled mast cells with intracellular MHCII (light blue), LAMP (orange), and acidification probe (red). Representative images shown at 30 min; 1000X magnification. (B) LVS (green) infected WT and TLR2$^{-/-}$ mast cell analysis by confocal microscopy at 3 h; c-Kit (purple), LAMP (orange), MHCII (light blue). (C) Bacterial enumeration (*F. tularensis* SCHU S4) of cellular lysates and active caspase-3 analysis by flow cytometry at 3 (white) and 24 h (solid bar). Unpaired t test *$p < 0.05$. Error bars represent the mean ±SD.
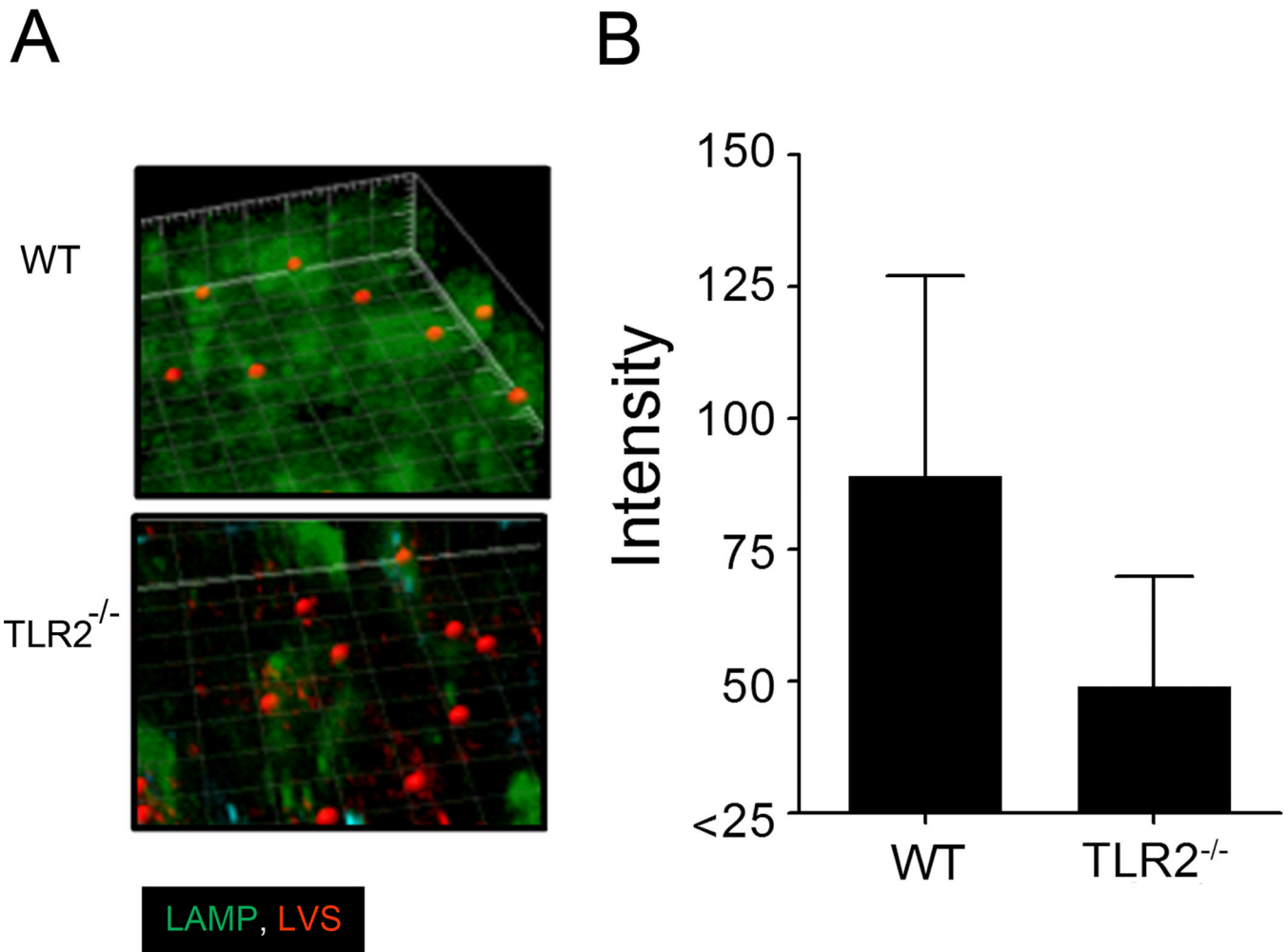
A

WT

TLR2$^{-/-}$

LAMP, LVS

B

Figure 5. Lung cell LAMP2 molecules encompass LVS (mCherry) during pulmonary infection
(A) Day 4 WT and TLR2$^{-/-}$ lung tissue shown. Representative 3D images shown with LAMP2 (green) and spot (red LVS regions of > 0.5 μm following bacterial challenge) analysis (400X magnification). (B) LAMP2 average intensity encompassing LVS positive regions (> 0.5 μm) of WT compared to TLR2 $^{-/-}$ lung tissue ($p < 0.005$).
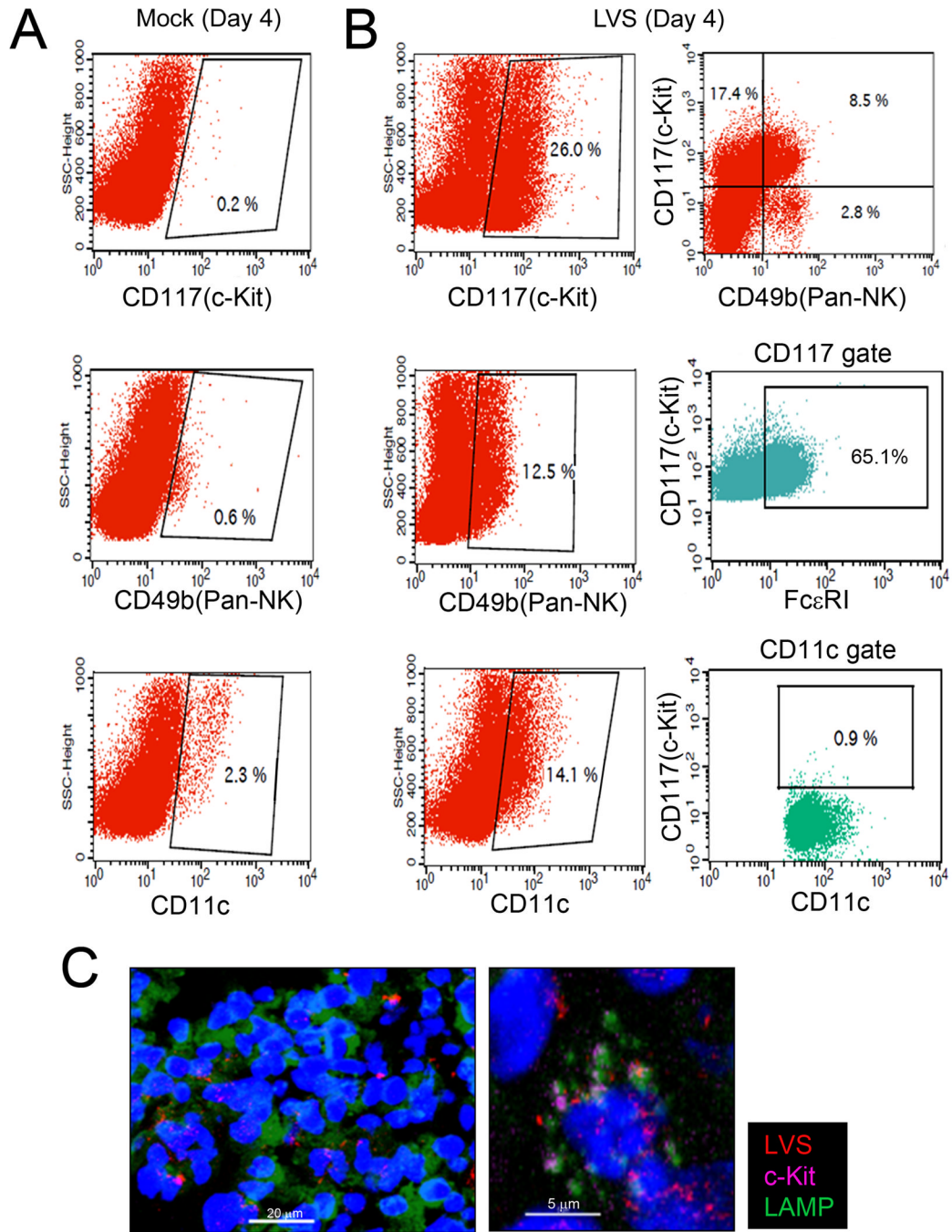
Figure 6. Mast cells infiltrate the lungs during pulmonary *F. tularensis* infection
Lungs cells from WT and TLR2$^{-/-}$ mice were analyzed at days 2 and 4 post-challenge (day 4 shown). Cells were surfaced stained with cKit, CD49b (panNK cell marker), and CD11c (dendritic cell marker) fluorochrome conjugated antibodies or isotype control. (A) Day 4 Mock: representative scatter plots shown with c-Kit gate, NK cell gate, and dendritic cell gate. (B) Day 4 LVS infected lung cells: c-Kit gate, NK cell gate; and dendritic cell gates ; c-Kit$^+$CD49b$^+$ NK cells (top right dot plot) with further analysis within c-Kit gate (middle dot plot) for double positive c-Kit$^+$FcεRI$^+$ mast cells and c-Kit$^+$CD11c$^+$ dendritic cells (bottom right dot plot). Samples were acquired with FACS Calibur (50K–100K cells) and analyzed with CellQuest. Representative scatter and dot plots shown for mock and LVS

infected lung cells. (C) Confocal microscopy analysis: c-Kit$^+$LAMP$^+$ cells (purple/green) in direct contact with mCherry LVS (KKF314); nucleus (DAPI, blue); representative confocal microscopy image (left) at 400X magnification with enlargement (right) shown.